J. Coat. Technol. Res., **18** (3) 627–639, 2021
https://doi.org/10.1007/s11998-021-00467-z

Roll-to-roll micromolding of UV curable coatings

Yuyang Du, Krystopher S. Jochem, Nitika Thakral, Alon V. McCormick, Lorraine F. Francis

Received: 1 September 2020 / Revised: 31 December 2020 / Accepted: 5 January 2021

Abstract In this study, fast and continuous fabrication of microscale structures by roll-to-roll UV imprinting or micromolding is demonstrated on a 121 mm wide web. This process is enabled by a UV curable thiol-ene-acrylate resin system, following the work of Stadlober and coworkers. A series of formulations were prepared with fast curing speeds at ambient conditions, low viscosities, and tunable mechanical properties. The rate and extent of curing as a function of the formulation composition were investigated with Fourier transform infrared spectroscopy. Consistent with the past work, we show that the thiol-ene-acrylate formulations reached high double bond conversions (> 80%) with the maximum conversion increasing with the relative thiol content and decreasing with the viscous urethane acrylate oligomer content. The double bond conversion of the patterned coatings (in contact with the mold) is shown to be ~ 80% for a range of UV lamp powers and web speeds up to 2.7 cm/s. Areas of the coating not covered by the mold required higher UV lamp power and/or lower web speeds to cure to a tack-free state. Microscale channels and arrays of recessed wells with various dimensions and pattern densities were continuously fabricated. Our findings show the successful use of a tetrafunctional thiol in the thiol-ene-acrylate resin system. We also discuss guidelines for the selection of processing conditions for the manufacturing of structured plastic substrates using roll-to-roll imprinting processes, opening up potential new applications.

Keywords Roll-to-roll micromolding, Thiol-ene, UV curing, High process throughput

Yuyang Du and Krystopher S. Jochem have contributed equally to this work.

Y. Du, K. S. Jochem, N. Thakral, A. V. McCormick (✉), L. F. Francis (✉)
Department of Chemical Engineering and Materials Science, University of Minnesota, 421 Washington Ave SE, Minneapolis, MN 55455, USA
e-mail: mccormic@umn.edu

L. F. Francis
e-mail: lfrancis@umn.edu

Introduction

Polymer films or coatings with surface nano-/microstructures are attracting research interest and finding a wide range of applications within optical films,[1] electronic devices,[2,3] and microfluidics.[4,5] Imprinting (also known as embossing or micromolding) is one of the most promising techniques for the mass production of structured polymer materials, offering both high resolution and low cost.[6] Ultraviolet (UV) imprinting is a particularly attractive option. In UV imprinting, a UV curable liquid is pressed with a mold or stamp and then cured with UV light. Starting from a low-viscosity liquid material, UV imprinting can be performed at room temperature and moderate pressures. Compared with thermal imprinting, an alternative imprinting process that involves time-consuming heating/cooling cycles, UV imprinting has greater potential in terms of process speed and pattern replication fidelity.[7–9] With a drum-based imprinting stamp, roll-to-roll (R2R) UV imprinting enables large-area and continuous fabrication of structured films, as demonstrated in the recent work by Jochem et al. for printed electronics[10] and Shan et al. for optical devices.[11]

During the past decade, the development in R2R imprinting has enjoyed great momentum. Guo et al. pioneered the research in pilot-scale R2R nanoimprinting on flexible substrates, demonstrating the continuous fabrication of patterns for wire-grid polarizers with features down to 70 nm from a UV curable epoxysilicone material.[12] Furthermore, they presented

a thorough investigation on the residual layer thickness of imprinted coatings as a function of the web speed and the applied force.[13] Carter and his group reported R2R imprinting at sub-100 nm resolution with a commercial UV curable resin[14] and successfully fabricated infrared sensors by subsequent deposition of carbon nanotubes.[15] Peng and coworkers reported the implementation of anodic aluminum oxide molds in R2R nanoimprinting and the fabrication of multiscale features, achieving polymer surfaces with both antireflective and hydrophobic properties.[16] Recently, our research group has used R2R UV imprinting of a commercial UV resin along with inkjet printing to fabricate metal electrical conductors[10] and electrical resistors.[17]

These studies suggest the industrial potential of R2R imprinting, but currently available UV curable materials are limited. Most previous studies are based on traditional UV curable materials: acrylates and epoxies. Acrylate materials cure fast and are readily available with a large number of monomers and oligomers. However, acrylates are known to suffer from oxygen inhibition and require inert atmospheres for high process speeds.[18] In addition, the volume shrinkage of acrylates during curing can be as high as 10%, leading to loss of pattern accuracy and defects due to internal stress buildup. The curing of epoxies is not inhibited by oxygen and the volume shrinkage is smaller after curing, but the reaction speed is much lower compared with acrylates.[19–21] Another concern with epoxy materials in imprinting is their strong adhesion, which may lead to demolding failures and defects in replicated patterns.

Thiol-ene chemistry, as an alternative UV curable system, cures as fast as acrylates under ambient conditions with less shrinkage.[22] Few previous studies have reported on the application of thiol-ene coatings in R2R imprinting.[23] Carter and coworkers fabricated superhydrophobic coatings based on multifunctional thiol and ene monomers.[24] Recently, Stadlober and coworkers demonstrated the application of the thiol-ene-acrylate ternary system in R2R nanoimprint lithography (NIL) processing and achieved the replication of multilength scale patterns at high accuracy and process speed.[25] The UV curable coatings were formulated based on urethane-acrylate oligomers, low-viscosity acrylates, and thiol monomers. By adjusting the ratios between oligomers, acrylates, and thiols, they demonstrated the versatility of this system by preparing formulations that had adjustable viscosities, fast UV curing behavior, and reduced sensitivity to oxygen, and producing final cured materials with elastic moduli ranging from 50 MPa to 5 GPa. Moreover, they showed that the addition of fluoropolymers reduced the surface energy of the UV-cured coatings and therefore enhanced the surface replication in the R2R NIL process.

This paper aims to further explore the thiol-ene-acrylate system for R2R imprinting to produce microstructured plastic substrates and investigate the effects of processing parameters and imprint stamp coverage on the extent of cure of the patterned coating (Fig. 1). We are particularly interested in microstructured substrates for R2R printed electronics.[2,3,10,17] In this application, fast curing systems that produce mechanically robust and high-resolution patterns are needed. The extent of cure of imprinted films and coatings is of great importance from both processing and application perspectives. Insufficient cure of coatings leads to a lower modulus and results in permanent deformation during the demolding step. Additionally, residual reactive species in the patterned polymers can migrate to the surface over time, leading to long-term stability issues and raising potential health concerns. We demonstrate continuous and large-area R2R imprinting with a UV curable thiol-ene acrylate-based coating system using formulations related to those demonstrated by Stadlober and coworkers.[25] Using a high-intensity UV light source, the UV curable formulations were varied to attain maximum achievable conversions at ambient conditions within seconds. The curing extents were analyzed with Fourier transform infrared spectroscopy (FTIR) as a function of the lamp power, the lamp distance, and the web speed. The conversion of patterned coatings remains high with increasing web speed and decreasing lamp power (UV dose) to the limits we explored with R2R processing. Microscale surface patterns with various shapes and dimensions were successfully fabricated on a 121 mm wide flexible web at a web speed up to 2.7 cm/s.

Experimental

Materials

Figure 2 shows the chemical structure of materials utilized in these UV curable formulations, adapted from the formulation described by Stadlober and coworkers.[25] Ebecryl 8210 was a tetrafunctional urethane acrylate oligomer (UAO) ordered from Allnex. Hexanediol diacrylate (HDDA) was provided by Sartomer. Pentaerythritol tetrakis(3-mercaptopropironate) (PETMP) and 2,2-dimethoxy-2-phenylacetophenone (DMPA) were purchased from Sigma-Aldrich. We note that our thiol oligomer is tetrafunctional, unlike the tri- and monofunctional thiols described by Stadlober and coworkers.[25] All the materials were used as received. For comparison, NOA-73, a thiol-ene-based optical adhesive from Norland Optical Adhesives, was used as a commercial benchmark for comparison in roll-to-roll imprinting studies.

Table 1 summarizes the compositions of liquid formulations with mole percentages shown based on the total amount of functional groups (the thiol group and double bonds). All the formulations contain 3 wt% of DMPA as photoinitiator. All the components were added to a glass vial wrapped with aluminum foil and

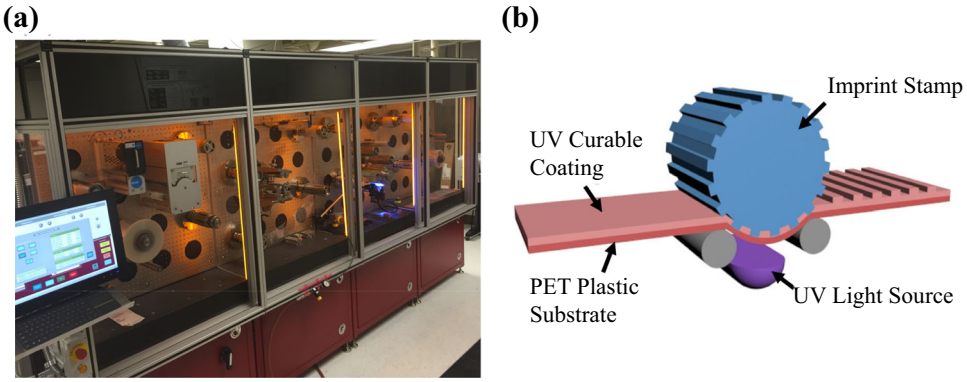

Fig. 1: (a) R2R UV imprinting line at the University of Minnesota. (b) Schematic of the R2R UV imprinting process

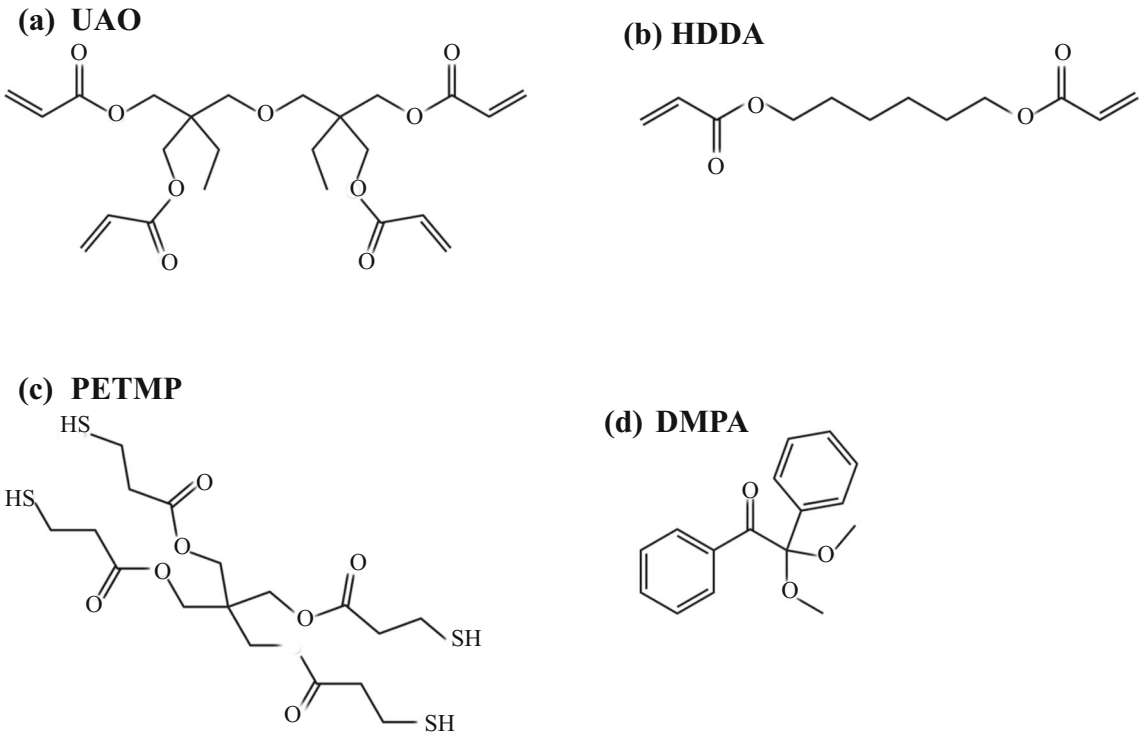

Fig. 2: Materials of R2R UV micromolding coating formulations: (a) principal component of Ebecryl 8210 (UAO), (b) hexanediol diacrylate (HDDA), (c) pentaerythritol tetrakis(3-mercaptopropironate) (PETMP), and (d) 2,2-dimethoxy-2-phenylacetophenone (DMPA)

Table 1: Compositions of R2R UV micromolding formulations

Formulation	PETMP (mol%)	HDDA (mol%)	UAO (mol%)
15-85_UAO50	15	42.5	42.5
20-80_UAO50	20	40	40
25-75_UAO50	25	37.5	37.5
30-70_UAO50	30	35	35
50-50_UAO50	50	25	25
20-80_UAO25	20	60	20
20-80_UAO75	20	20	60

stirred for 4 h at room temperature. In the nomenclature for the formulation, taking 15-85_UAO50 for example, ''15'' stands for the percentage of thiol functional groups of total reactive functional groups, ''85'' stands for the double bond percentage (including those from both HDDA and UAO) of total reactive functional groups, and ''50'' is the percentage of the double bond from UAO.

Dynamic viscosity

The dynamic viscosity of liquid coating formulations was measured on an AR-G2 rheometer (TA Instruments). The parallel plate geometry was used with a plate diameter of 25 mm and a gap of 1 mm. The measurements were performed at room temperature with the shear rate ranging from 1 to 100 s^{-1}.

FTIR spectroscopy

The curing kinetics of UV curable formulation were analyzed with a Nicolet 6700 FTIR spectrometer in transmission mode. A thin layer of UV curable liquid coating was coated on a sodium chloride plate by a Mayor rod. The coating was exposed to the air during measurement. The coating thickness before UV curing was 20 μm. Samples were exposed to UV light at 500 mW/cm^2 with a mercury lamp (OmniCure 1500, Excelitas Technologies) inside the IR chamber. The UV light source is the same as that on the R2R imprinting line. A series of IR spectra were taken at a sample interval of 0.02 s. The spectrometer was operated at a resolution of 32 and 1 scan per spectrum.

The conversion of cured samples from the R2R experiment was determined with FTIR-ATR spectroscopy. Cured samples were placed in contact with a diamond crystal on the FTIR spectrometer. The peak areas of thiol (2570 cm^{-1}) and acrylate double bond (1635 and 1619 cm^{-1}) were analyzed and normalized using the carbonyl IR peak (1725 cm^{-1}) as an internal reference. The conversion (x) of a functional group (thiol groups or double bonds) was determined by using equation (1):

$$x = \frac{A_0 - A_t}{A_0} \times 100\% \quad (1)$$

where A_0 is the peak area before curing and A_t is that after curing.

Dynamic mechanical analysis

Dynamic mechanical analysis was conducted on an RSA-G2 solid analyzer (TA Instruments) with a tension fixture. Samples were cured materials with dimensions of 20 mm (length) × 5 mm (width) × 0.18 mm (thickness). Curing conditions were UV curing at 500 mW/cm^2 for 2 min followed by thermal cure at 120°C overnight in an oven. It is important to note that these conditions provide significantly more UV dosage than was applied during R2R experiments. A temperature ramp was performed from 25 to 200°C at a heating rate of 3°C/min and a frequency of 1 Hz. The oscillation strain was 0.02% and was allowed for autoadjustment from 0.001 to 3%.

Preparation of PDMS mold

PDMS imprinting molds were prepared from master patterns fabricated on 4-inch diameter silicon wafers prepared by traditional photolithography processes using SU-8 photoresist. These patterns consisted of parallel raised lines and square dots 10 μm in depth, the lateral dimensions of which range from 10 to 80 μm. Thirty grams of liquid PDMS (Sylgard 184, Dow Corning) at 10:1 base/curing agent by weight was mixed thoroughly and vacuum degassed to remove all air bubbles. The liquid PDMS was then poured over the silicon wafer master pattern in a petri dish and cured at 75°C for 2 h in an oven before demolding. The PDMS was then thermally annealed at 120°C for 2 h and 210°C for 2 h. The cured PDMS stamps were secured to a piece of silicone-coated PET (Hotpress) using PDMS mixed at a 10:4 base/curing agent ratio as an adhesive. The assembled stamp was then cured for 24 h at 45°C. After curing, the stamp was clamped to the imprinting roll, using the procedure given by Jochem et al.[10]

R2R imprinting or micromolding

R2R imprinting was performed on a commercial R2R nanoimprinting machine from Carpe Diem Technologies. A clear 127 μm thick polyethylene terephthalate (PET) web was unwound and passed through a web cleaner. Then, reverse gravure coating was used to deposit a 25 μm thick layer of the UV curable resin onto the web. The coated web then passed to the imprinting station where web tension pressed the UV curable resin into the features of the imprinting stamp as the coated web passed around the imprinting drum. Web tension was maintained at 8.9 N during the imprinting process, and speed was varied to test imprinting conditions. While the web passed around the imprinting drum, it was illuminated through the PET web with a mercury arc lamp UV light source as illustrated in Fig. 8. The light from the UV light source (OmniCure S1500) is directed to the web through a light guide and slab illuminator positioned at the base of the imprinting drum to illuminate a strip across the web as shown in Fig. 8. There are no filters in the OmniCure system, but no information is known about filtering of the light by the light guide. The light intensity at the coating is controlled both with the lamp

intensity and with the distance of the lamp from the web (increasing the sight angle, and consequently the length over which the light shines, as described later in this work). The total UV dose is controlled by the intensity of the UV light source and by the web speed. After curing, the web was delaminated from the imprinting roll and rewound on a collection roll.

Results and discussion

Formulation characterization

We used UV curable coating formulations based on four main components, as described by Stadlober and coworkers.[25] A tetrafunctional thiol monomer, PETMP, was selected due to its fast cure and the capability to reduce oxygen inhibition. A tetrafunctional urethane acrylate oligomer (UAO) was selected because of its high functionality, which typically leads to a high cure speed, and its relatively low viscosity compared with other acrylate oligomers. In addition, an acrylate monomer, hexanediol diacrylate was used as a reactive diluent to reduce the formulation viscosity to facilitate mold filling. Lastly, DMPA was used as the photoinitiator to induce photopolymerization. Two sets of formulations were prepared to develop an optimized coating for R2R UV imprinting applications. In the first set of formulations, the molar ratio between thiol groups and double bonds (i.e., the thiol-to-ene ratio) was varied from 15:85 to 50:50, with the molar ratio of double bonds from UAO kept at 50% for all formulations. In the second set of formulations, the molar ratio between UAO and the acrylate monomer was varied while the thiol to double bond ratio was constant.

Three criteria were considered for R2R UV imprinting optimization: liquid coating viscosity, cure speed, and cured material modulus. A relatively low viscosity is beneficial to promote mold filling, but too low a viscosity can decrease the liquid coating thickness deposited on the web by reverse gravure coating in our system. Insufficient resin on the web can lead to defects where mold features are not fully filled. High UV cure speeds are extremely beneficial, as achieving sufficient cure is often the bottleneck preventing increased processing speed. Insufficient extent of cure can leave the pattern tacky and excess free monomers in the coating, which could interfere with intended uses of the patterned coatings. Furthermore, the modulus of the cured coating, which is a function of the extent of cure, must be high enough to withstand the mechanical deformation during demolding since this can cause permanent damage to imprinted features. At the same time, a certain extent of flexibility is necessary to allow for the release of surface microstructures from the mold without damage to the mold.

Characteristics of liquid formulations

As shown in Fig. 3, all the tested formulations are Newtonian liquids in the range of shear rates investigated. The coating viscosity was adjustable over a range from 0.03 to 0.32 Pa s in ways consistent with the data shown by Stadlober and coworkers.[25] Here we have chosen formulations for low viscosity. Viscosity was found to increase with the thiol content (and hence decrease with the amount of low-viscosity HDDA component) from $\sim$ 0.07 Pa s for 15-85_UAO50 to $\sim$ 0.12 Pa s for 50-50_UAO50. Viscosity also strongly increases with the UAO content as shown in Fig. 3b, as expected based on the higher viscosity of the oligomer compared to the other components.[25] This viscosity range is comparable to commercial UV curable resists and much lower than those of polymer melts during thermal imprinting.[26,27]

Curing kinetics

Curing kinetics are of great importance to R2R UV imprinting applications because high cure speeds enable high-throughput production and sufficient cure extents are required to address safety concerns, and increase the hardness of cured materials and long-term stability. In thiol-ene chemistry, the curing kinetics are influenced by the functionality of monomers and oligomers, the reactivity of functional groups, the ratio of thiol-to-ene functional groups, the viscosity of formulations, and the photoinitiator properties.[28,29] In this research, monomers and oligomers with high functionalities and reactivities were selected to formulate coating materials. The ratio between different components was adjusted to investigate the effects of thiol-to-ene ratio and the coating viscosity on curing behaviors.

To quantitatively investigate how the curing speed and extent vary with different formulations, real-time FTIR was performed on the aforementioned coating formulations at a UV intensity comparable to that used on the R2R imprinting line, i.e., 500 mW/cm^2. The UV light was turned on 5 s after the start of IR spectrum collection. Both the thiol group and the double bond conversion were analyzed according to their characteristic IR peaks at 2570 and 810 cm^{-1}, respectively.

In Fig. 4a, the double bond conversion is plotted against the exposure time for coatings with various concentrations of thiol groups, ranging from 15% (for 15-85_UAO50) to 50% (for 50-50_UAO50) based on the molar ratio of functional groups. All the coating formulations react almost instantly upon UV exposure, reaching the limiting or ultimate conversion within several seconds. As the thiol-to-ene ratio increases, both the reaction speed and the limiting conversion of double bonds increase. Providing more PETMP drives the conversion of the double bonds to completion. Therefore, the double bond conversion increases as the thiol concentration increases. For the 50-50_UAO50

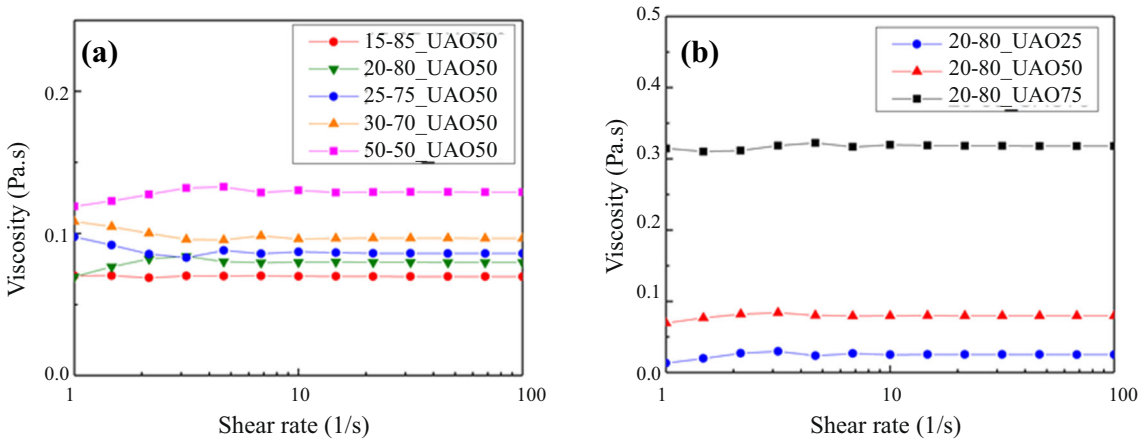

Fig. 3: (a) Dynamic viscosity for coating formulations with different ratios of thiol groups and acrylate double bonds. (b) Dynamic viscosity for formulations with various UAO contents

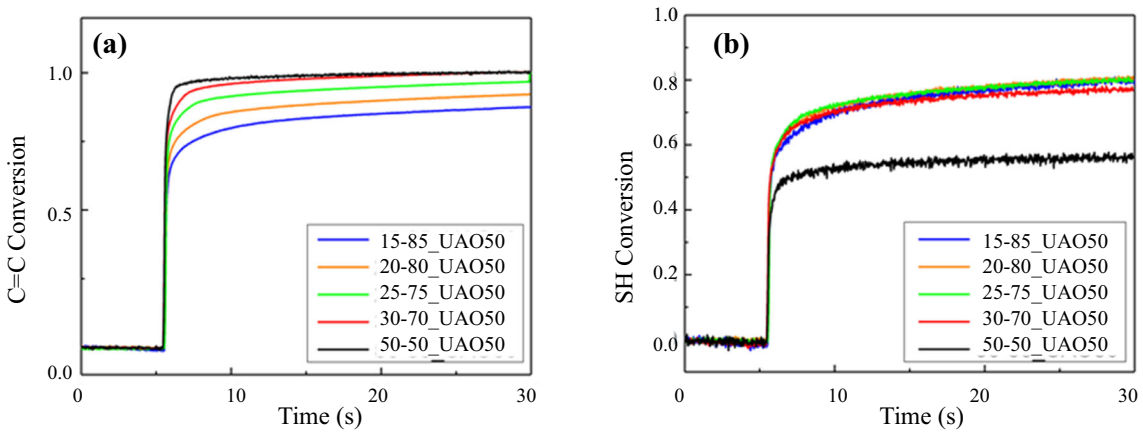

Fig. 4: (a) Double bond conversion and (b) thiol group conversion for formulations with different thiol-to-ene ratio recorded by real-time FTIR at a light intensity of 500 mW/cm^2. The relative ratio between UAO and HDDA was kept constant. Coatings (20 μm thick) were exposed to air

formulation, the thiol conversion is lower than the formulations with less initial thiol content. A portion of the acylates homopolymerize, leading to insufficient double bonds available for the thiol-acrylate reaction and preventing complete conversion of the thiols. Similar trends were observed in previous studies on thiol-ene curing kinetics under light intensities two orders of magnitudes lower.[30] The presence of thiol accelerates the reaction of acrylate double bonds by reducing the oxygen inhibition effects.[31] Moreover, Cramer and Bowman demonstrated that thiol helps encourage full acrylate conversion through the action of chain transfer, preventing radical trapping, and possibly also by plasticizing the growing network.[32] These trends are consistent with those shown by Stadlober and coworkers.[25]

According to Fig. 4b, the thiol groups were sufficiently cured with a conversion of about 80% except for the formulation containing 50% thiol groups (50-50_UAO50), which is due to the competition between the thiol-acrylate reaction and the acrylate homopolymerization.[32] For UV curable thiol-acrylate formulations, a thiol group concentration around 30% appears to be optimal for both the reaction rate and curing extent considerations. With this concentration of thiol groups, maximum SH and C=C conversion is reached in the shortest period of time.

Another series of thiol-acrylate formulations was prepared with a constant thiol-acrylate ratio (20% thiol group) but various UAO-to-HDDA ratios. In the nomenclature of formulations, the number following UAO indicates the percentage of double bonds from UAO out of the total amount of double bonds. According to Fig. 5, all the formulations exhibit high cure speeds, a steep rise in conversion in the first 1–2 s of UV exposure followed by a slower increase in conversion over the following 5 s, and high final conversion of all groups on the multifunctional monomers, suggesting a highly crosslinked polymer network. However, the limiting conversions of double bonds and thiol groups slightly decrease with increasing UAO oligomer concentration. This could be

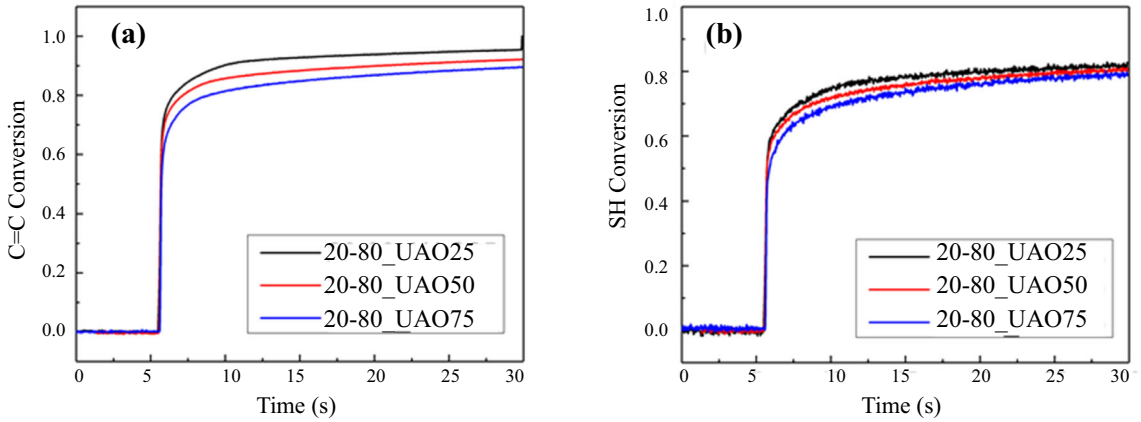

Fig. 5: (a) Double bond conversion and (b) thiol group conversion for coating formulations with various UAO content under UV intensity of 500 mW/cm^2. The thiol-to-ene ratio was kept constant. Coatings are 20 μm thick and exposed to air during the measurement

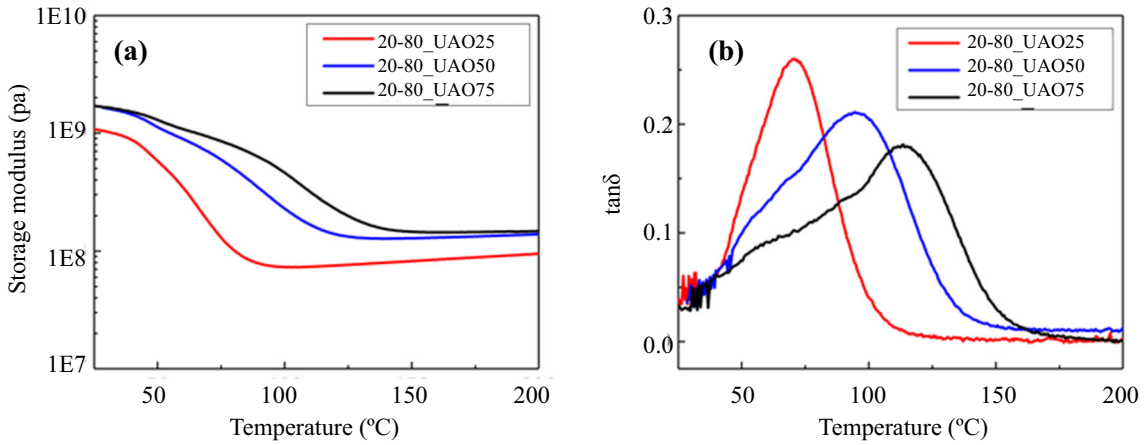

Fig. 6: (a) Storage modulus, *E′*, and (b) tanδ as a function of temperature for cured materials with different UAO concentrations. Samples were UV cured at 500 mW/cm^2 for 2 min followed by thermal curing at 120°C overnight in an oven

explained by the high viscosity of the oligomer restricting the mobility of propagating radicals.[25]

Overall, for the prepared thiol-ene-acrylate formulations, the achievable conversion increases with an increase in the relative thiol content and a decrease in the UAO content. In spite of these differences, all formulations reached the plateau conversions within seconds under UV illumination and the changes in the formulation are not expected to change the achievable conversion significantly, with all the double bond conversions higher than 80%.

Mechanical properties of cured materials

Figure 6 shows the temperature-dependent viscoelastic properties of cured coating formulations with various UAO content. The three formulations have the same thiol-to-ene ratio (20% thiol groups) and the percentage of double bonds from UAO was varied from 25 to 75%. After curing, the materials develop high elastic moduli of 1–2 GPa at room temperature and exhibit glass transition temperatures higher than room temperature, indicating the formation of hard and glassy materials. According to Fig. 6a, the plateau storage modulus at high temperatures increases with the UAO content, suggesting a higher effective crosslink density. The higher functionality of the UAO may contribute to this increase;[33] however, the plateau modulus of the 20-80_UAO75 cured polymer is only slightly higher than that of the 20-80_UAO50 polymer. From the tanδ curves shown in Fig. 6b, the T_g values were 75, 95, and 115°C for formulations containing 25%, 50%, and 75% UAO double bonds, respectively. The cured material is therefore a relatively homogeneous network with a single glass transition temperature, as expected from the compatibility of the polymer segments. However, tanδ peaks broaden as UAO content increases, sug-

gesting a decreasing degree of homogeneity due to the heavily crosslinked polymer networks.[34] This heterogeneity may be part of the result of radical trapping and cyclization associated with the multifunctional acrylate, commonly observed in multifunctional chain polymerizations and consistent with the decreasing acrylate fractional conversion shown in Fig. 5a. In the R2R imprinting process, as discussed below, demolding takes place at room temperature. Therefore, the high T_g, together with the high strength of the cured thiol-ene, can significantly improve the mechanical integrity of surface microstructures, permitting defect-free demolding of imprinted coatings.

R2R UV micromolding

Effects of thiol and oligomer contents on conversions

R2R UV micromolding experiments were performed with thiol-ene-acrylate coating formulations. All the formulations were coated onto a PET web using a reverse microgravure roll coating unit, forming a uniform liquid coating on a PET web. The imprinting roll was wrapped with a PDMS mold with a microscale regular pattern. The thiol-ene-acrylate-coated PET web was pressed against the imprinting roll by web tension, which imprints the coating with the pattern. Due to the relatively low viscosities of thiol-ene-acrylate formulations (see Fig. 3), the mold cavities were successfully filled without significant bubble defects in the cured coating. A high-intensity UV light source cures the resin while the resin is in contact with the mold. Since the coated portion of the web was wider than the patterned mold and some resin was also squeezed out to the edge of the mold, a portion of the resin was not covered by the mold when it was exposed to the UV light. The cured coatings were delaminated from the mold without any problems, attributed to the low surface energy of the PDMS mold and the sufficient mechanical strength of cured materials.

The extent of cure of the UV micromolded coating was characterized with FTIR-ATR and plotted against the web speed. Due to a limited penetration depth of the ATR technique (ca. 1 μm from the coating surface) and the relatively small amounts of thiol groups in the formulation, the thiol peaks were noisy and thus not employed for the analysis in this section. The curing extents of micromolded coatings are represented by the double bond conversion and plotted against the web speed in Fig. 7.

All coating formulations were sufficiently cured over the range of web speeds investigated since the extent of cure always exceeded 85% and surfaces were tack-free. According to Fig. 7a, the limiting double bond conversion increases as the thiol-to-ene ratio increases and is independent of web speed over this range. This result is similar to the trend observed in the real-time kinetics study shown in Fig. 4a and suggests that the addition of thiol monomers facilitates the curing of acrylates, which could be attributed to reduced oxygen inhibition effects and increased chain transfer. However, the limiting conversion values of imprinted coatings measured by ATR (Fig. 7a) were slightly lower compared with those measured in the transmission mode (Fig. 4a) for the same formulation, respectively. The observed difference may come from the characterization technique and a depth-wise conversion gradient. The ATR data represent the coating surface conversion while, in the FTIR technique, the average conversion throughout the coating thickness is characterized. Therefore, it is suggested that the surface conversion was slightly lower, which could be attributed to two sources. First, since the UV exposure is from the back side of the coated plastic web during the roll-to-roll micromolding experiments and the UV curable resin absorbs some of the incident UV energy, the top surface of the resin receives a lower UV dosage than the bottom, which may lead to reduced conversion at the top surface relative to the bottom. In addition, oxygen inhibition may also be a source of lower surface conversion. Oxygen could diffuse into the surface of the UV curable resin layer as it traveled from the coating station to the imprinting stamp or from the PDMS stamp into the surface of the UV curable resin during molding, leading to reduced surface conversion. As discussed previously, the thiol conversion was not complete in a stoichiometric mixture of thiol and ene groups (50-50_UAO50) although the double bond conversion was higher. The thiol-ene ratio was kept at 30 to 70 when investigating the oligomer contents with R2R micromolding.

As shown in Fig. 7b, lowering the oligomer content in the formulation raises the double bond conversion. As discussed below, there is a trend to lower conversions as the web speed increases. With the formulation containing 25% oligomer (30-70_UAO25), a web speed of 2.7 cm/s was achieved at high pattern fidelity while at the same time maintaining a high curing extent (85% conversion of double bonds). At similar starting concentrations of functional groups, the formulation with a lower viscosity (30-70_UAO25) achieves higher conversion, likely due to an enhanced molecular mobility of reactive species. Furthermore, the conversion is more complete for coatings with lower modulus and lower T_g, which suggests loosely crosslinked polymer networks might allow for rearrangement of functional groups after solidification. In comparison, the attainable web speed for sufficient curing extent (tack-free surface) was 0.17 cm/s with a commercially available optical adhesive (NOA73) under the same imprinting conditions, which is 15 times slower than the thiol-ene-based formulation developed in this work.

Effects of processing variables on conversion

The extent of cure during the R2R micromolding process is crucial to the successful fabrication of the surface microstructures, the integrity and mechanical

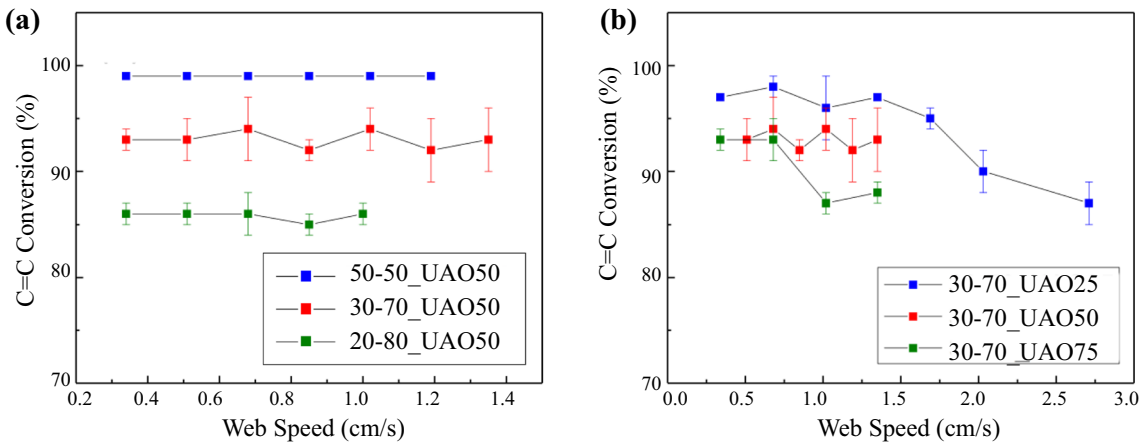

Fig. 7: Double bond conversions of thiol-ene-acrylate coatings plotted against the web speed of R2R micromolding for (a) formulations with different thiol-to-ene ratios and (b) formulations with different oligomer contents. Conversions were measured with FTIR-ATR on the top surface of the coating in contact with mold and averaged over three parallel measurements

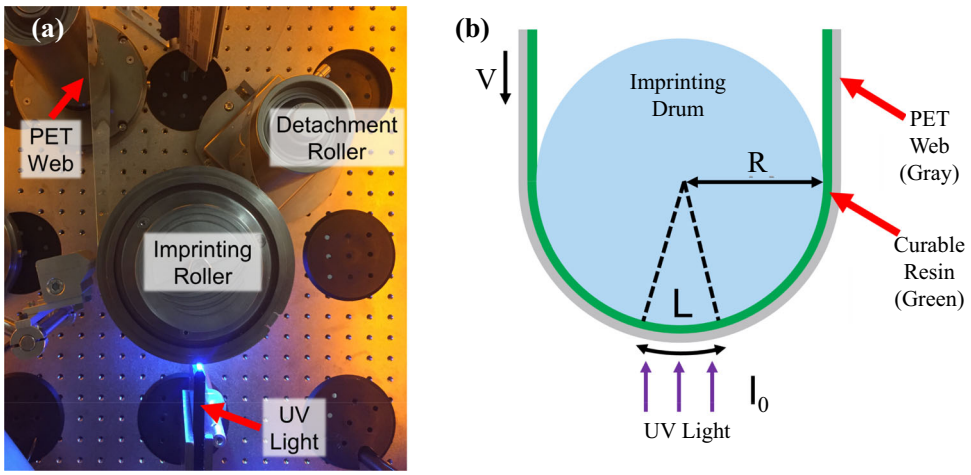

Fig. 8: (a) UV imprinting unit of the R2R imprinting line. (b) Schematic of the imprinting unit showing direction of web movement (*V*), direction of UV illumination (I_0), length of UV illuminated web (*L*), and imprinting drum radius (*R*). Parameters shown are those used in equation (1)

properties of the patterned surface, and the long-term stability of the cured coating.[7] The curing extent is determined by the UV dosage received by the coating, which can be estimated as shown in equation (2):

$$J = \frac{I_0 L}{V} \tag{2}$$

Here, J is the curing dosage, I_0 is the incident light intensity averaged along the web length, V is the web velocity, and L is the length of UV exposure area on the imprint stamp (shown in Fig. 8b). This expression assumes that the intensity is uniform through the thickness due to the low thickness and low photoinitiator content.[35] The photoinitiator, DMPA, shows an absorption peak at 365 nm (UVA). In general, the PET film absorbs UV in this region. The percentage of UV irradiance loss depends on the film thickness and the presence of additional UV filters. In this study, the PET film is free of additional UV filters and the thickness is relatively low. Therefore, the UV intensity change due to the PET film has been neglected (<10% based on experience).

The influence of incident light intensity on the double bond conversion of the imprinted coating was investigated with FTIR-ATR. As the lamp power was varied from 40 to 100%, the average UV intensity, I_o, was measured and found to increase proportionally with the lamp power from 220 to 500 mW/cm^2 and hence the dose also increased. As shown in Fig. 9a, different conversions were observed across the cured coating: the area in contact with the mold reached a plateau conversion at the lowest lamp power, and in contrast, the areas not in contact with the mold needed

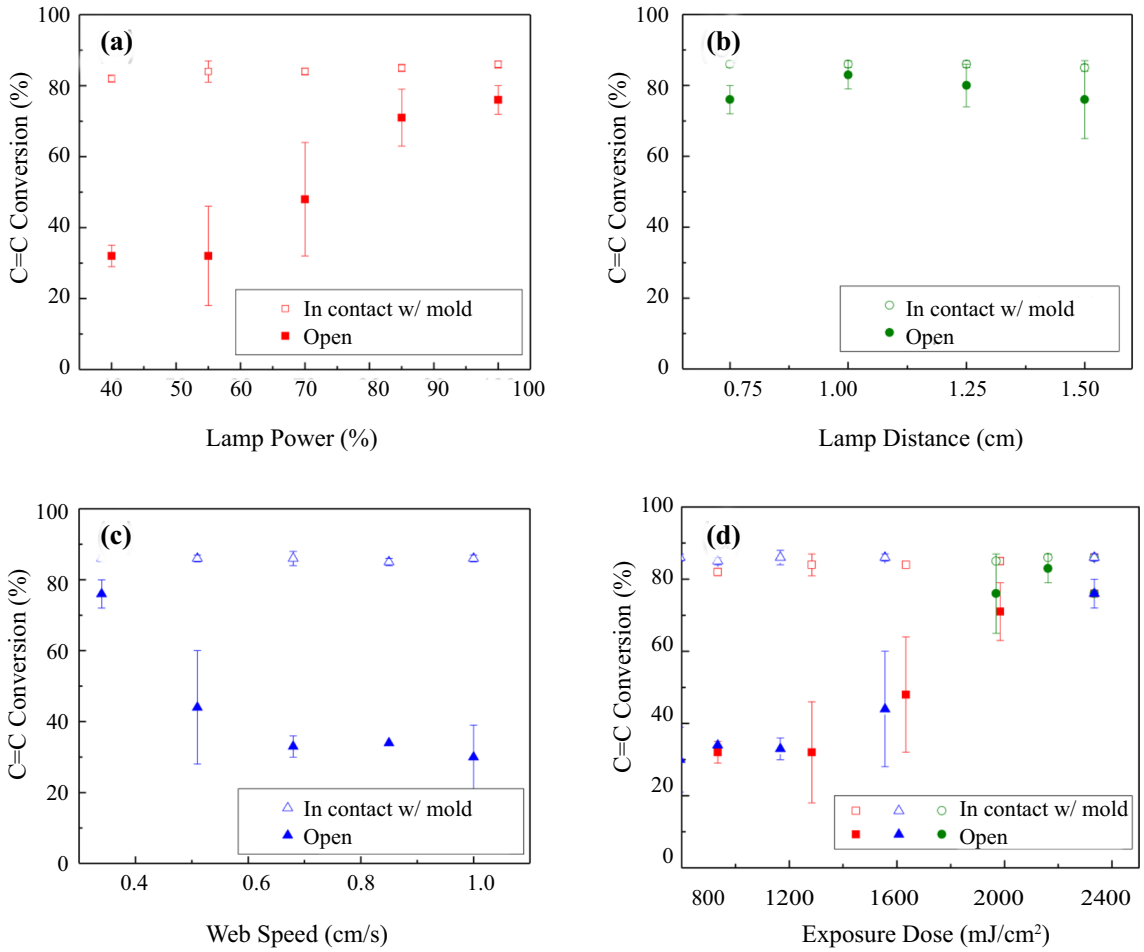

Fig. 9: (a) Effect of lamp power on conversion of micromolded coatings at a lamp distance of 0.75 cm and a web speed of 0.34 cm/s. (b) Effect of lamp distance on the imprinted coating conversion at a lamp power of 100% and a web speed of 0.34 cm/s. (c) Effect of web speed on the imprinted coating conversion at a lamp power of 100% and lamp distance of 0.75 cm. (d) Effect of exposure dosage on the imprinted coating conversion. The effects of lamp power, lamp distance, and web speed are included in the plot. For all plots, open symbols correspond to coatings cured in contact with the mold and the solid symbols correspond to the edges of the coatings, which were not covered by the mold and hence cured in air

a much higher lamp power, likely due to oxygen scavenging of radicals in the exposed regions. In the presence of oxygen, increasing the intensity leads to not only a faster initiation rate but also suppressed oxygen inhibition due to the faster viscosity increase, both of which contribute to the strong dependence of conversion on UV intensity.

A set of experiments was carried out to confirm that the lamp distance has no effect on dose and hence conversion of imprinted coatings. As the distance from the lamp to the coating was varied from $\sim$ 0.75 to $\sim$ 1.5 cm, the incident UV intensity decreased from $\sim$ 500 to $\sim$ 220 mW/cm^2 and the illuminated web length increased from $\sim$ 1.6 to $\sim$ 3.1 cm. The lamp distance affects the UV light distribution but not the total UV dosage. The double bond conversions as a function of lamp distance for the area in contact with mold and the open area are constant, as shown in Fig. 9b.

The effect of web speed on the imprinted coating conversion at constant UV intensity was studied. As shown in Fig. 9c, the patterned area of coating (in contact w/ mold) is sufficiently cured (nontacky) at all web speeds investigated. However, the unpatterned area of the coating (open) was tacky at web speeds over 0.5 cm/s with the corresponding double bond conversion decreasing significantly from 80% at 0.34 cm/s to 30% at 0.68 cm/s and remaining near that level as speed increased further. As web speed increases, the exposure time and hence UV dosage decreases. As discussed above, the open coating required higher UV doses to cure due to oxygen inhibition and hence the condition for sufficient (nontacky) cure was achieved only at lower speeds (higher doses).

According to equation (2), the UV dosage is approximately equal to $\frac{I_0 L}{V}$ for a specific coating system in the R2R imprinting process. Considering all the data

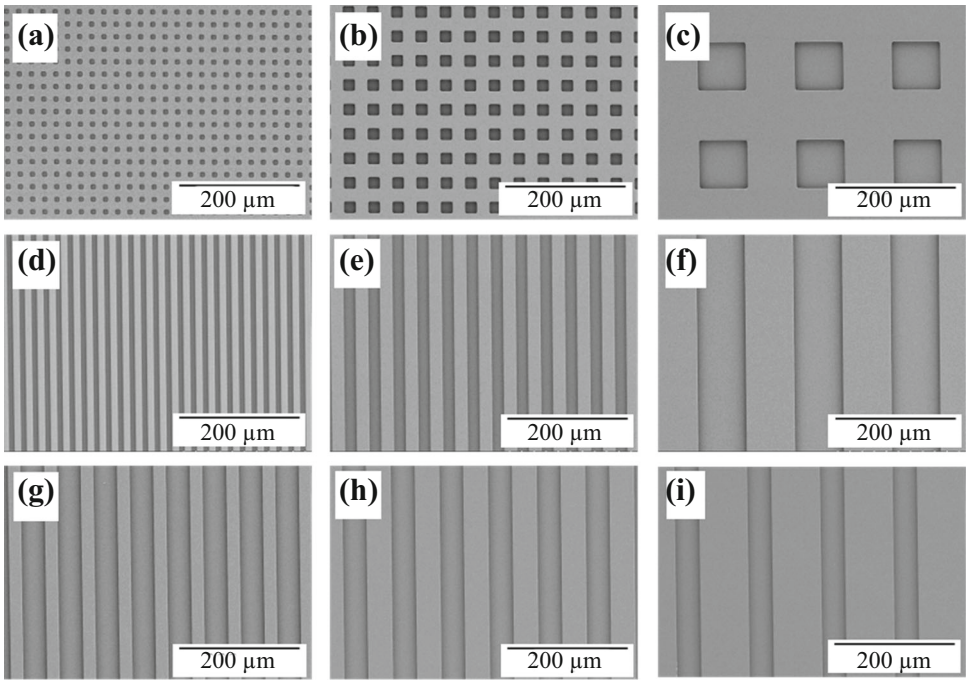

Fig. 10: R2R imprinting fabricated patterns with the 30-70_UAO25 coating formulation: (a–c) square recessed wells with pattern widths of 10, 20, 80 μm, respectively; (d–f) microchannel arrays with channel widths of 10, 20, 80 μm, respectively, and width/spacing = 1:1 for all three patterns, imprinted parallel to the web direction; (g–i) microchannel arrays with width/spacing = 2:1, 1:1, and 1:2, respectively, a channel width of 40 μm for all three patterns, imprinted parallel to the web moving direction. All the surface microstructures were 10 μm in depth

together, as shown in Fig. 9d, the conversion of the open regions is determined by the exposure dosage, while the conversion of regions that are in contact with the mold is at its maximum, independent of dose. The critical exposure dose for the coating system to reach the plateau conversion is less than $\sim$ 800 mJ/cm^2 on the area in contact with the mold. For the area of coating cured in air, the critical dose climbed significantly to $\sim$ 2000 mJ/cm^2 due to oxygen inhibition. For a given intensity and illuminated web length, the achievable web speed can be estimated with the critical exposure dosage. Comparing to a commercial UV curable resin (NOA-73), the thiol-ene-acrylate formulations allow for a higher achievable web speed (2.7 cm/s) due to the lower critical exposure dose. As shown in previous work, the achievable web speed of NOA-73 is approximately 0.17 cm/s under similar UV imprinting processing conditions.[10] Additionally, it should be mentioned that coating material that spreads outside the mold shows lower conversions because of oxygen inhibition. Slower speeds are necessary to fully cure this material, indicating the need to design molds to minimize spreading outside of the mold or add a nitrogen blanket to eliminate this effect.

Continuous fabrication of microstructured coatings

The patterning process was successfully scaled up on the R2R UV imprinting line. The 30-70_UAO25 formulation was selected for the fabrication of microstructured coatings and a web speed of 2.7 cm/s was used, resulting in fully cured patterned regions (not exposed to air). The use of a low-viscosity formulation and simple patterns oriented to encourage displacement of air during mold filling resulted in excellent pattern replication, but there was a sporadic incidence of bubble defects. Our recent work on the imprinting process shows that the addition of an air knife at the contact point between the coated web and the imprinting roll leads to further improvements in replication and a decrease in entrapped air defects.[10] Figure 10 shows SEM images of surface microstructures; various shapes, square recesses, and channels were replicated. The patterns are 10 μm in depth, and the lateral dimensions range from 10 to 80 μm. The pattern replication from the drum-based imprint stamp to the UV curable thiol-ene-acrylate coating was excellent, indicating the promise for R2R micromolding processes based on these formulations for applications in printed electronics,[10,17] for example.

Conclusions

In this study, the continuous fabrication of microstructured coatings with UV curable thiol-ene-acylate formulations was demonstrated. The liquid viscosity and the elastic modulus of cured materials were

tunable over a wide range by adjusting the thiol-to-ene ratio and the oligomer content. This finding is in agreement with the principles of the formulations shown by Stadlober and coworkers.[25] All the coating formulations cured fast under UV exposure, achieving high double bond conversions, ca. 80%, within seconds. High-speed R2R imprinting was achieved with the formulated thiol-ene-acrylate coatings at ambient conditions. The limiting double bond conversion was found to increase when increasing the thiol-to-ene ratio and decreasing the urethane acrylate content. In addition, the effects of R2R processing variables on the curing conversions for a representative coating formulation were investigated. FTIR results revealed that the curing extent in air increased with the UV exposure dose, which is proportional to the light intensity and the exposure length and inversely proportional to the web speed. The maximum achievable web speed with the custom thiol-ene-acrylate formulations was 2.7 cm/s, which is approximately 15 times greater than that of a commercial product (NOA73) under the same processing conditions.

Acknowledgments This work was supported by the Industrial Partnership for Research in Interfacial and Materials Engineering (IPRIME), University of Minnesota, and by the National Science Foundation (NSF Award No. CMMI-1634263). Parts of this work were performed at the Nano-Fabrication Center and the Characterization Facility, University of Minnesota, which receives partial support from NSF through the MRSEC program. We are grateful to Wieslaw Suszynski for the help with the R2R imprinting equipment. We thank Dr. Bing Luo and Dr. David Giles for the helpful discussion on FTIR measurement and DMA testing, respectively, and Dr. Boran Zhao for reviewing the manuscript. Krystopher Jochem gratefully acknowledges support from the NSF Graduate Research Fellowship Program under Grant No. (00039202).

References

1. Wu, H, Gao, J, Yi, P, Peng, L, Lai, X, ''Investigation of Reflective Performance for Micro-Pyramid Arrays by Roll-to-Roll UV Imprinting Process.'' *Microelectron. Eng.,* **182** 61–67 (2017)
2. Hyun, WJ, Zare Bidoky, F, Walker, SB, Lewis, JA, Francis, LF, Frisbie, CD, ''Printed, Self-Aligned Side-Gate Organic Transistors with a Sub-5 μm Gate-Channel Distance on Imprinted Plastic Substrates.'' *Adv. Electron. Mater.,* **2** (12) 1600293 (2016)
3. Mahajan, A, Hyun, WJ, Walker, SB, Rojas, GA, Choi, J-H, Lewis, JA, Francis, LF, Frisbie, CD, ''A Self-Aligned Strategy for Printed Electronics: Exploiting Capillary Flow on Microstructured Plastic Surfaces.'' *Adv. Electron. Mater.,* **1** (9) 1500137–1500146 (2015)
4. Wang, J, Ahmad, H, Ma, C, Shi, Q, Vermesh, O, Vermesh, U, Heath, J, ''A Self-Powered, One-Step Chip for Rapid, Quantitative and Multiplexed Detection of Proteins from Pinpricks of Whole Blood.'' *Lab Chip,* **10** (22) 3157–3162 (2010)
5. Kolliopoulos, P, Jochem, K, Lade, RK, Francis, LF, Kumar, S, ''Capillary Flow with Evaporation in Open Rectangular Microchannels.'' *Langmuir,* **35** (24) 8131–8143 (2019)
6. Liddle, JA, Gallatin, GM, ''Nanomanufacturing: A Perspective.'' *ACS Nano,* **10** (3) 2995–3014 (2016)
7. Schift, H, ''Nanoimprint Lithography: An Old Story in Modern Times? A Review.'' *J. Vac. Sci. Technol. B Microelectron. Nano. Struct.*, **26** (2) 458–480 (2008)
8. Neisser, M, ''Patterning Roadmap: 2017 Prospects.'' *Adv. Opt. Technol.,* **6** (3–4) 143–148 (2017)
9. Guo, LJ, ''Nanoimprint Lithography: Methods and Material Requirements.'' *Adv. Mater.,* **19** (4) 495–513 (2007)
10. Jochem, KS, Suszynski, WJ, Frisbie, CD, Francis, LF, ''High-Resolution, High-Aspect-Ratio Printed and Plated Metal Conductors Utilizing Roll-to-Roll Microscale UV Imprinting with Prototype Imprinting Stamps.'' *Ind. Eng. Chem. Res.,* **57** (1) 16335–16346 (2018)
11. Shan, XC, Liu, T, Mohaime, M, Salam, B, Liu, YC, ''Large Format Cylindrical Lens Films Formed by Roll–to–Roll Ultraviolet Embossing and Applications as Diffusion Films.'' *J. Micromech. Microeng.,* **25** (3) 035029 (2015)
12. Ahn, SH, Guo, LJ, ''High-Speed Roll-to-Roll Nanoimprint Lithography on Flexible Plastic Substrates.'' *Adv. Mater.,* **20** (11) 2044–2049 (2008)
13. Ahn, SH, Guo, LJ, ''Large-Area Roll-to-Roll and Roll-to-Plate Nanoimprint Lithography: A Step Toward High-Throughput Application of Continuous Nanoimprinting.'' *ACS Nano,* **3** (8) 2304–2310 (2009)
14. John, J, Tang, Y, Rothstein, JP, Watkins, JJ, Carter, KR, ''Large-Area, Continuous Roll-to-Roll Nanoimprinting with PFPE Composite Molds.'' *Nanotechnology*, **24** (50) (2013)
15. John, J, Muthee, M, Yogeesh, M, Yngvesson, SK, Carter, KR, ''Suspended Multiwall Carbon Nanotube-Based Infrared Sensors via Roll-to-Roll Fabrication.'' *Adv. Opt. Mater.,* **2** (6) 581–587 (2014)
16. Peng, L, Zhang, C, Wu, H, Yi, P, Lai, X, Ni, J, ''Continuous Fabrication of Multiscale Compound Eyes Arrays With Antireflection and Hydrophobic Properties.'' *IEEE Trans. Nanotechnol.,* **15** (6) 971–976 (2016)
17. Cao, M, Jochem, KS, Hyun, WJ, Francis, LF, Frisbie, CD, ''Self-Aligned Inkjet Printing of Resistors and Low-Pass Resistor—Capacitor Filters on Roll-to-Roll Imprinted Plastics with Resistances Ranging from 10 to to 10^6 Ω.'' *Flex. Print. Electron.,* **3** 045003–045012 (2018)
18. Studer, K, Decker, C, Beck, E, Schwalm, R, ''Overcoming Oxygen Inhibition in UV-Curing of Acrylate Coatings by Carbon Dioxide Inerting Part I.'' *Prog. Org. Coat.,* **48** (1) 92–100 (2003)
19. Cai, Y, Jessop, JLP, ''Decreased Oxygen Inhibition in Photopolymerized Acrylate/Epoxide Hybrid Polymer Coatings as Demonstrated by Raman Spectroscopy.'' *Polymer (Guildf),* **47** (19) 6560–6566 (2006)
20. Park, YJ, Lim, DH, Kim, HJ, Park, DS, Sung, IK, ''UV- and Thermal-Curing Behaviors of Dual-Curable Adhesives Based on Epoxy Acrylate Oligomers.'' *Int. J. Adhes. Adhes.,* **29** (7) 710–717 (2009)
21. Sangermano, M, Malucelli, G, Delleani, G, Priola, A, ''Bicyclo-Orthoester as a Low-Shrinkage Additive in Cationic UV Curing.'' *Polym. Int.,* **56** 1224–1229 (2007)
22. Du, Y, Xu, J, Sakizadeh, JD, Weiblen, DG, McCormick, AV, Francis, LF, ''Modulus- and Surface-Energy-Tunable Thiol-

Ene for UV Micromolding of Coatings.'' *ACS Appl. Mater. Interfaces,* **9** (29) 24976–24986 (2017)
23. Du, Y, Xu, J, Sakizadeh, J, McCormick, A, Francis, L, ''Scalable Fabrication of Microstructured Coatings with Thiol-Ene Photopolymers and UV Led Curing.'' *Abstr. Pap. Am. Chem. Soc.*, **254** (2017)
24. Li, Y, John, J, Kolewe, KW, Schiffman, JD, Carter, KR, ''Scaling Up Nature: Large Area Flexible Biomimetic Surfaces.'' *ACS Appl. Mater. Interfaces,* **7** (42) 23439–23444 (2015)
25. Leitgeb, M, Nees, D, Ruttloff, S, Palfinger, U, Götz, J, Liska, R, Belegratis, MR, Stadlober, B, ''Multilength Scale Patterning of Functional Layers by Roll-to-Roll Ultraviolet-Light-Assisted Nanoimprint Lithography.'' *ACS Nano,* **10** (5) 4926–4941 (2016)
26. Hirai, Y, Yoshikawa, T, Takagi, N, Yoshida, S, Yamamoto, K, ''Mechanical Properties of Poly-Methyl Methacrylate (PMMA) for Nano Imprint Lithography.'' *J. Photopolym. Sci. Technol.*, **16** 615–620 (2003)
27. Yi, P, Wu, H, Zhang, C, Peng, L, Lai, X, ''Roll-to-Roll UV Imprinting Lithography for Micro/Nanostructures.'' *J. Vac. Sci. Technol. B, Nanotechnol. Microelectron. Mater. Process. Meas. Phenom.*, **33** (6) 060801 (2015)
28. Jian, Y, He, Y, Jiang, T, Li, C, Yang, W, Nie, J, ''Volume Shrinkage of UV-Curable Coating Formulation Investigated by Real-Time Laser Reflection Method.'' *J. Coat. Technol. Res.,* **10** (2) 231–237 (2013)
29. Hoyle, CE, Bowman, CN, ''Thiol-Ene Click Chemistry.'' *Angew. Chem. Int. Ed.,* **49** (9) 1540–1573 (2010)
30. Senyurt, AF, Wei, H, Hoyle, CE, Piland, SG, Gould, TE, ''Ternary Thiol-Ene/Acrylate Photopolymers: Effect of Acrylate Structure on Mechanical Properties.'' *Macromolecules,* **40** (14) 4901–4909 (2007)
31. O'Brien, AK, Cramer, NB, Bowman, CN, ''Oxygen Inhibition in Thiol-Acrylate Photopolymerizations.'' *J. Polym. Sci. Part A Polym. Chem.*, **44** (6) 2007–2014 (2006)
32. Cramer, NB, Bowman, CN, ''Kinetics of Thiol-Ene and Thiol-Acrylate Photopolymerizations with Real-Time Fourier Transform Infrared.'' *J. Polym. Sci. Part A Polym. Chem.*, **39** (19) 3311–3319 (2001)
33. McNair, OD, Sparks, BJ, Janisse, AP, Brent, DP, Patton, DL, Savin, DA, ''Highly Tunable Thiol-Ene Networks via Dual Thiol Addition.'' *Macromolecules,* **46** (14) 5614–5621 (2013)
34. Jin, K, Wilmot, N, Heath, WH, Torkelson, JM, ''Phase-Separated Thiol-Epoxy-Acrylate Hybrid Polymer Networks with Controlled Cross-Link Density Synthesized by Simultaneous Thiol-Acrylate and Thiol-Epoxy Click Reactions.'' *Macromolecules,* **49** (11) 4115–4123 (2016)
35. Payne, JA, Francis, LF, McCormick, AV, ''The Effects of Processing Variables on Stress Development in Ultraviolet-Cured Coatings.'' *J. Appl. Polym. Sci.,* **66** (7) 1267–1277 (1997)